CREEP STRENGTH AND STRUCTURAL STABILITY OF WELD JOINTS OF CREEP RESISTANT FERRITIC STEELS

Dagmar Jandová, Josef Kasl, Václav Kanta

ŠKODA VÝZKUM s.r.o., Tylova 57, Plzeň 316 00, Czech Republic

dagmar.jandova@skodavyzkum.cz

Figure 1. Macrostructure of C weld joint after PWHT

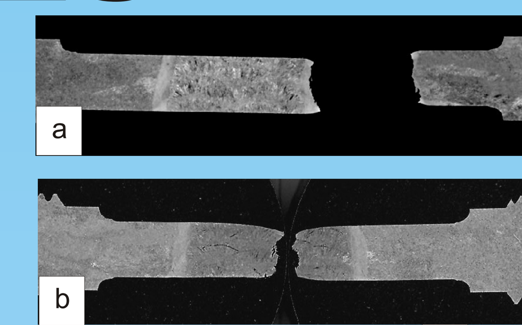

Figure 2. Macrostructure of crept samples of C weld joint: a) 600°C/80MPa/25,818hrs and b) 625°C/50MPa/29,926hrs

Introduction

Turbines, boilers and steam piping belong to the most exposed parts of steam power plants. They have been operating under severe service conditions for several decades. Therefore high mechanical strength, good corrosion/oxidation resistance and high structural stability of materials used for their production are desired. High chromium ferritic steels are preferred for high creep strength and low cost. However, long-term results show a significant drop of their creep strength and overestimation of service life at high temperatures. From this point of view long term creep testing of the base materials and welded joints is of a great importance. Welds are usually characterized with a high structural heterogeneity and increased susceptibility to fracture in comparison to the base materials.

High creep strength of chromium ferritic steels is caused by four contributions to the strengthening: (1) substructural strengthening of chromium rich M23C6 carbides, which are pinning grain and subgrain boundaries, (ii) precipitation strengthening of fine vanadium (V,Nb)N nitrides, (ii) substitutive strengthening of solid solution by molybdenum and/or tungsten atoms and (iv) dislocation strengthening. During creep exposures two main processes occur: recovery and precipitation of secondary phases that can result in changes of creep strength.

The study deals with investigation of four trial weld joints which satisfied requirement according to welding standards and were used for production of the steam piping and cast components of steam turbine. The following base materials were used for welding: P91 steel - the main representative of creep resistant modified 9Cr-1MoV steels, which is currently used for manufacturing of components operating at temperatures up to 585°C, P92 steel - 9Cr-1/2MoWV developed for utilization at ultra-supercritical conditions of steam at temperatures up to 625°C and P22 steel - 21/4Cr-1Mo steel, used in creep conditions up to 525°C, exceptionally up to 540 °C.

The objectives of study

1. Determination of the creep strength of the weld joints for 100,000 hrs at different temperatures ranged from 525 to 650°C.
2. Determination of critical zones from the point of view of the creep failure.
3. Study of microstructural changes taking place during creep exposures.
4. Elucidation of the creep failure mechanism in dependency on creep conditions.

Table 1. Chemical composition of the base materials and weld metals (weight %)

	C	Mn	Si	Cr	Mo	V	Ni	Nb	Al	N	P	S	W
BM P91 plate	0.12	0.41	0.21	8.8	0.92	0.22	0.10	0.09	0.004	0.06	0.014	0.008	-
WM weld C	0.12	0.71	0.23	9.1	1.05	0.20	0.68	0.05	0.005	0.04	0.012	0.009	-
BM P91 pipe	0.12	0.49	0.29	8.6	0.96	0.21	0.30	0.07	0.011	0.06	0.011	0.004	-
WM weld C1	0.12	0.70	0.21	9.1	1.05	0.21	0.73	0.05	0.003	0.04	0.010	0.006	-
BM P22 pipe	0.11	0.46	0.25	2.24	0.95	-	-	-	-	-	0.013	0.002	-
WM weld C2	0.06	0.70	0.22	2.22	0.99	-	-	-	-	-	0.012	0.01	-
BM P92 pipe	0.12	0.41	0.25	8.6	0.47	0.17	0.11	0.06	0.029	0.045	0.015	0.003	1.75
WM weld C3	0.13	0.61	0.24	8.93	0.99	0.18	0.67	0.07	0.005	0.041	0.007	0.002	1.55

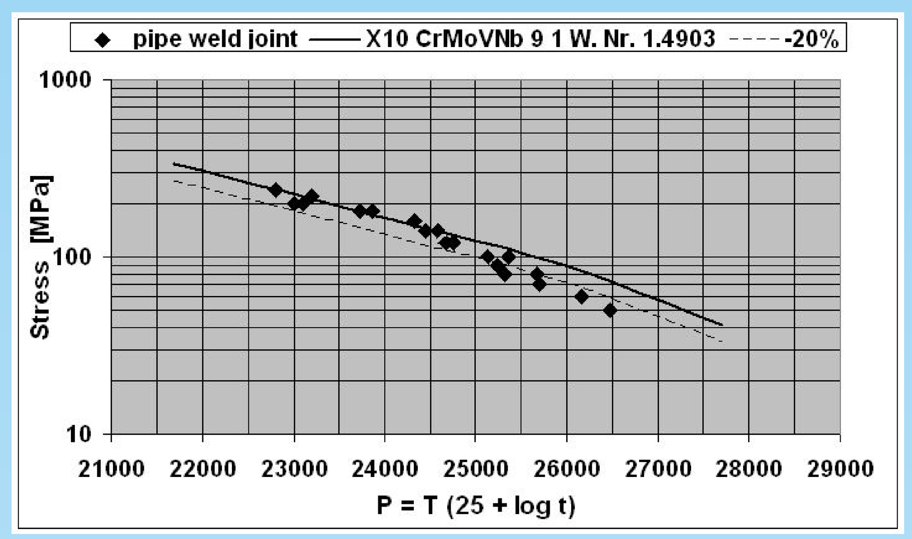

Figure 3. The creep rupture strength of the similar pipe weld joint (C1 weld joint) in comparison to the creep strength of the base material (wrought P91 steel X10CrMoVNb 9 1 W)

Experimental procedures

Four trial weld joints were produced using GTAW & SMAW welding method:
C weld - the similar plate weld joint of P91 steel (Fig. 1),
C1 weld - the similar pipe weld joint of P91 steel,
C2 weld - the dissimilar pipe weld joint of P22 and P91 steels,
C3 - the similar pipe weld joint of P92 steel.
The first weld joint was produced of the cast plates of P91 steel with dimensions of 500 x 150 x 25 mm that were welded together in PA position. The pipe weld joints were joined in PC position using segments of 325 mm outer diameter, 25 mm wall thickness and 400 mm length. The chemical compositions of the base materials and the weld metals are given in Table 1. The heat treatment of the base materials: P91 steel - 1050°C/1.5hrs/ oil + 750°C/3.5 hrs, P22 steel - (920°C960)°C/air + (680°C750)°C, P92 steel - 1060°C/1.5hrs/oil + 770°C/3.5 hrs. The post-weld heat treatment (PWHT) was applied: (740750°C)/2.5hrs for the C weld joint, 760°C/2.5hrs for the C1 weld joint, 730°C/2,5hrs for the C2 weld joint and 760°C/4hrs for the C3 weld joint. Creep testing to rupture of smooth cross-weld specimens (Fig. 2) were performed (16 samples of the C, 19 of the C1 and 15 of the C2 weld joint, 12 of the C3 weld joint). Creep data were evaluated in dependency of Larson-Miller parameter P=T.(C+logt), where T is temperature [K], C is a material constant (20 for P22 steel, 25 for P91 steel and 36 for P92 steel) and t is time to rupture [hrs]. The creep strengths of weld joints were compared to the creep strength of the base materials (Fig. 3). Fractures occurred in different zones in dependency of type of weldment and conditions od creep exposures (Fig. 4,5). Fractographic analysis of ruptured samples (Fig. 6) was carried out using scanning electron microscopy (SEM). Vickers hardness measurement across the weld joints was performed. Changes in hardness profiles (Fig. 9) indicated changes in mechanical properties in individual zones of weld joint, which were caused by microstructural processes taking place during high temperature exposures. Microstructure was investigated in order to elucidate causes of fracture in different zones of weld joint (Fig. 7). Cavitation failure (Fig. 8) and distribution of coarse particles of secondary phases were observed on metallographic samples using light microscopy (LM) and SEM (Fig. 11). Substructures before creep testing (Fig. 10) and after long creep exposures (Fig. 12 -15) were evaluated using transmission electron microscopy (TEM). Precipitates were identified using X-ray energy-dispersive microanalysis (EDX) and electron diffraction. Thin foils and extraction replicas were prepared from the weld metal (WM), the heat affected zones (HAZ) and the base material unaffected by welding (BM).

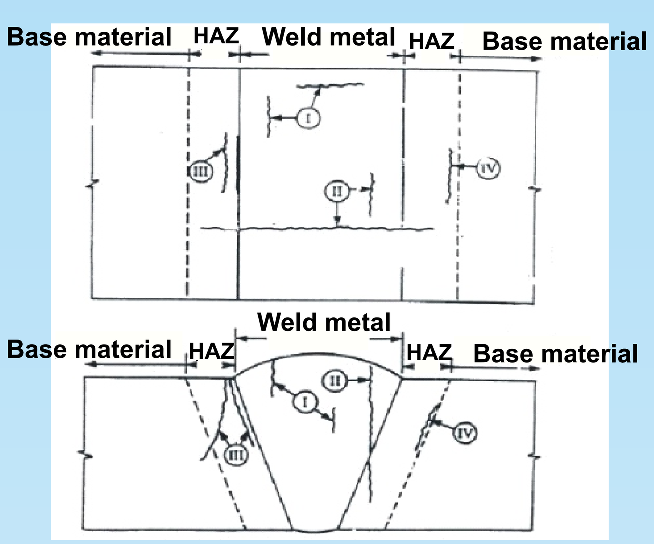

Figure 4. Classification of cracking of weld joints.

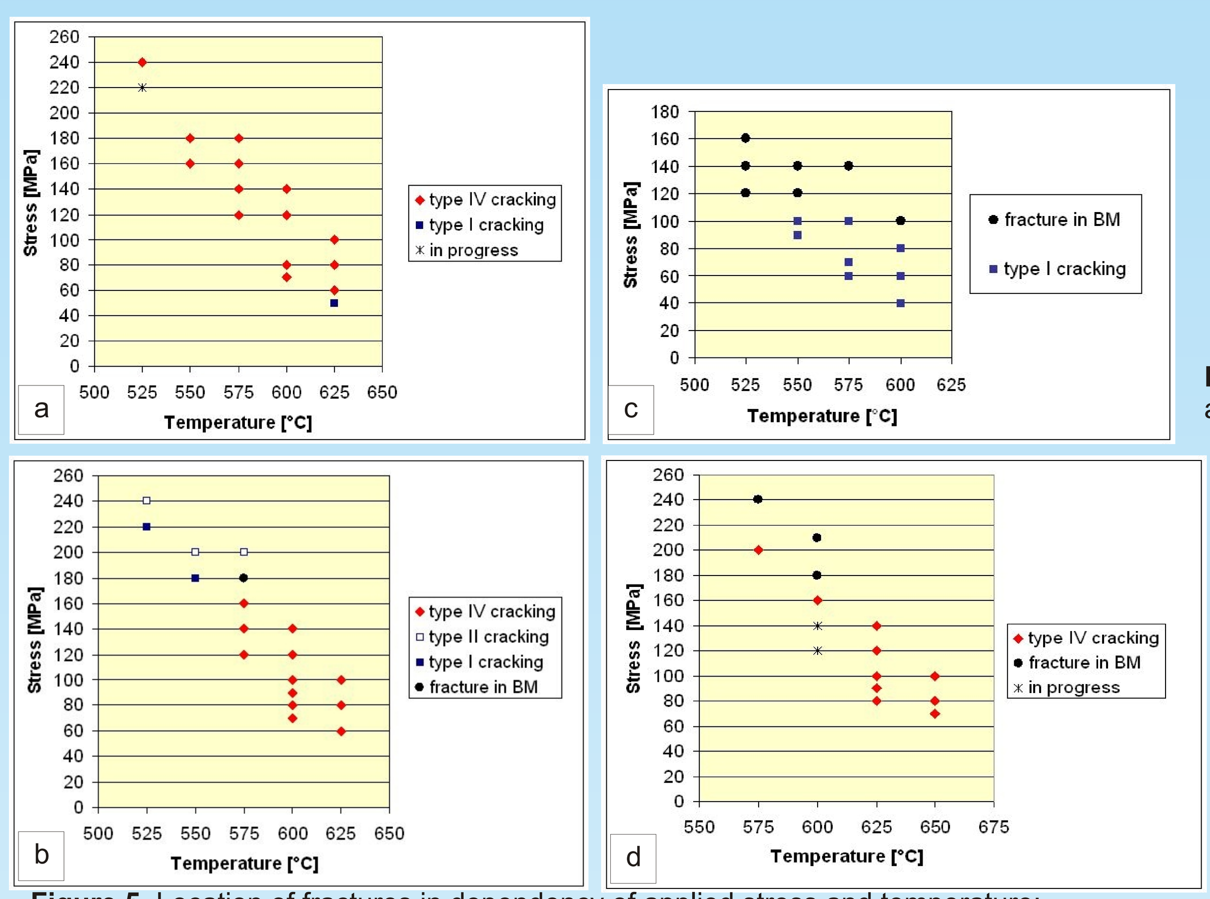

Figure 5. Location of fractures in dependency of applied stress and temperature: a) C weld point, b) C1 weld point, C2 weld point and d) C3 weld joint.

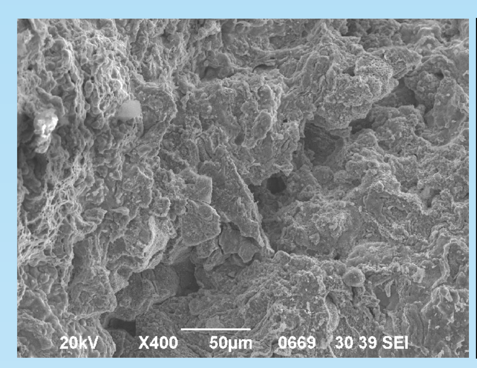

Figure 6. Fracture surface of C weld after test 625°C/50MPa/29,312hrs.

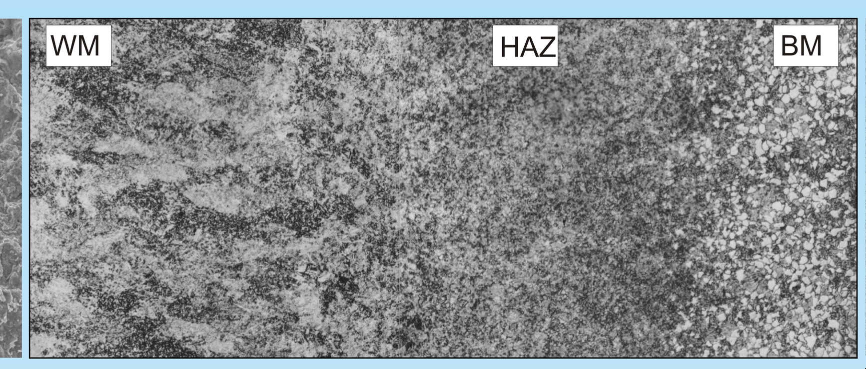

Figure 7. Microstructure of C2 weld joint after PWHT. LM micrograph.

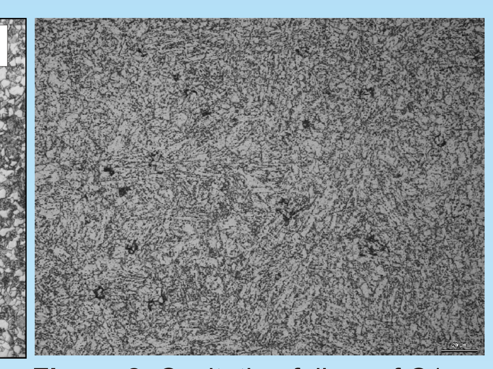

Figure 8. Cavitation failure of C1 weld joint, 625°C/50MPa/29,962hrs. LM micrograph.

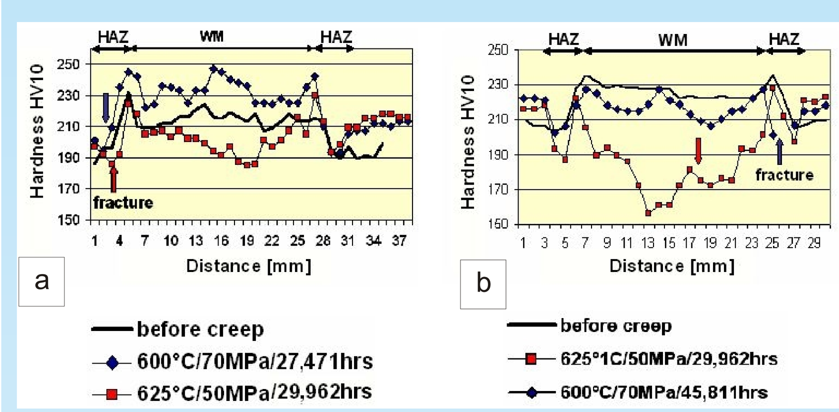

Figure 9. Hardness profiles across weldments after creep tests: a) C1 weld joint and b) C weld joint.

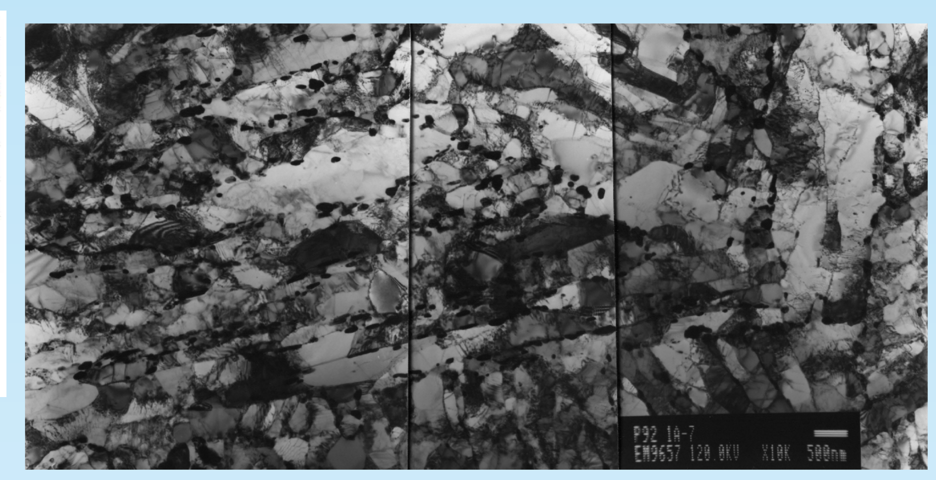

Figure 10. Substructure of the base material of C3 weld joint after PWHT. TEM micrograph.

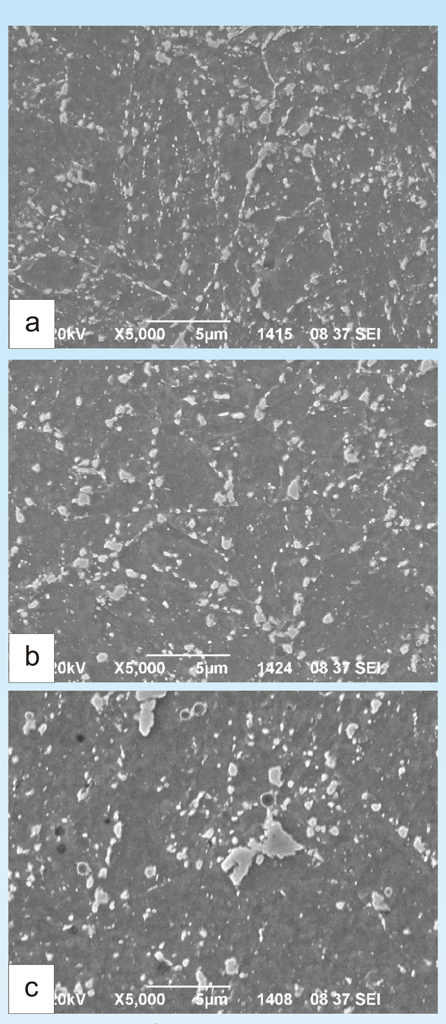

Figure 11. Secondary phases in ferritic matrix of C weld joint after test 625°C/50MPa/29,312hrs: a) the base material, b) fine grained HAZ and c) the weld metal. SEM micrograph.

Results and conclusions

At temperature ranges used in service creep strength of all weld joints investigated fell into ±20% scatter band of the creep strength of the base material that is usually permitted for welded pipes. The similar weld joints of P91 steel (C and C1 welds) satisfied these requirements for 100,000 hrs up to 575 °C [1-4], dissimilar P91 and P22 steel up to 550 °C [5,6]. Creep testing of P92 steel weld joint is still running nevertheless it seams that the creep strength of weld joint fulfils above mentioned requirement up to 600 °C. The creep strength of P92 steel weld joint is rather higher than that of P91 steel weld joints, however did not reach expected values [7,8]. Microstructure of C, C1 and C3 weld joint corresponded to tempered martensite, while microstructure of C2 consisted of tempered martensite (P91 steel), tempered bainite (the weld metal and HAZ of P22 steel) and annealed mixture of ferritic-perlitic structure (the base material of P22 steel unaffected by welding).
Fracture of C weld joint occurred I n the fine grained HAZ (type IV cracking) in almost the whole ranges of applied stresses and temperatures; only one sample tested at the highest temperature and the lowest stress ruptured in the weld metal. Fine grained HAZ is typical zone, where creep failure is concentrated during long creep exposures. The reason of this effect is relatively high density of coarse precipitates (mainly M23C6 carbides) and low density of fine VN precipitate. Contribution of precipitation strengthening was low, soft subgrains were plastically deformed; cavities were formed at boundaries that can growth thanks high grain boundary diffusion. After creep exposure at 625 °C for about 30,000hrs coarse particles of Fe2Mo Laves phase occurred especially in the weld metal as they often precipitated at the surface of oxide inclusions. Then solid solution was depleted about atoms of Mo and substitutive strengthening of solid solution significantly dropped. In addition, after such long exposures Z-phase nucleated. It is known that this Cr(V,Nb)N nitride can growth rapidly at high temperatures and cases dissolution of fine vanadium nitride. This effect results in decrease of precipitation strengthening after long exposures at temperatures above 550°C.
Times to rupture of C1 weld joint were not as long as of C weld joint. This was probably a result of too high temperature of PWHT. The strength of the weld metal was rather lower than in the C weld joint. At relatively low temperatures and high stresses fracture occurred by slip mechanism similar to rupture at room temperature. Then cracks propagated in the weld metal and type I and II fracture occurred. At higher temperatures dislocation creep predominated, cavitation failure was concentrated in fine grained HAZ and type IV fracture was observed. Laves and Z-phase were also observed but only exceptionally.
Fracture of C2 weld joint occurred at high stresses and lower temperature in the base material unaffected by welding, which consisted of relatively soft feritic-pearlitic structure. After long creep exposures differences between ferritic-pearlitic and bainitic structure gradually disappeared; microstructure consisted of featureless ferritic matrix with carbides. At higher temperatures and lower stresses the weld joint ruptured in the fine grained low alloyed bainitic zone in the weld metal. Large area of grain boundaries promoted formation and growth of cavities and crack propagation in this zone. High alloyed parts of the weldment were of relatively high creep strength.
The C3 weld joint revealed the highest creep strength. In tempered martensite high density of particles of secondary phases was observed: coarse M23C6 carbides and Laves phase and fine vanadium nitrides. After creep tests at temperatures above 575 °C slight coarsening of particles at grain/subgrain boundaries was found out while vanadium nitrides were stabile. Facture occurred in the base material unaffected by welding after application of highest stresses at relatively low temperatures for very short times. Other samples ruptured as usual in the fine grained HAZ.

Acknowledgements: This work was supported by Grant projects SMS 4771868401 and 1P05OC024 COST 536 the Ministry of Education, Youth and Sports of the Czech Republic.

References: list is in enclosed box.

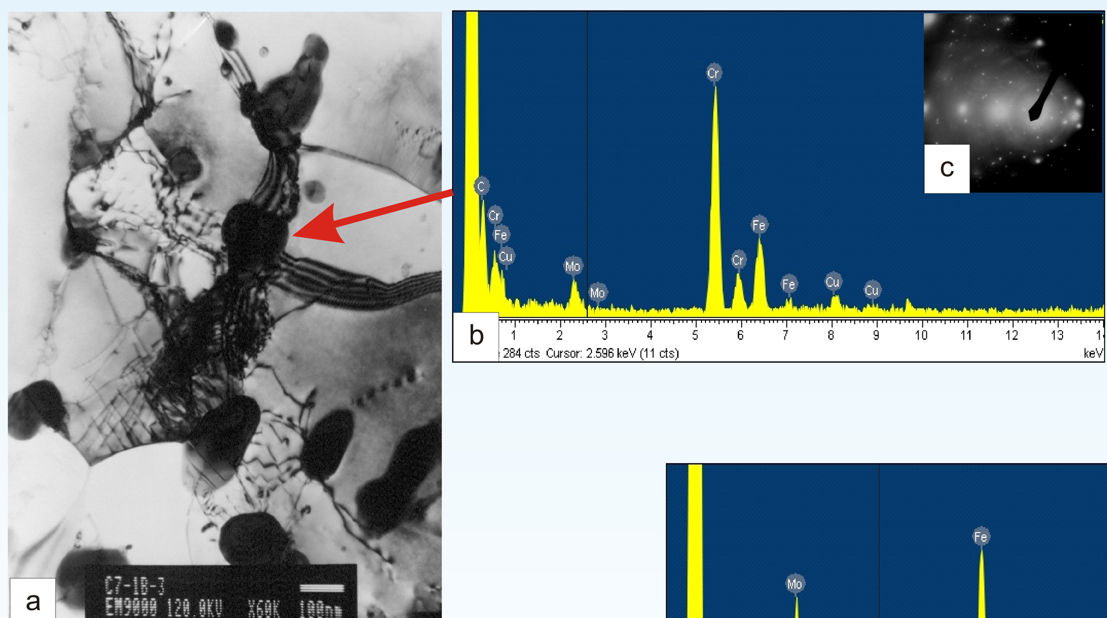

Figure 12. Coarse particles at grain/subgrain boundaries in the fine grained HAZ of C weld tested at 575°C/140MPa/10,031hrs: a)TEM micrograph, b) EDX spectrum and c) electron diffraction patterns of M23C6 carbides.

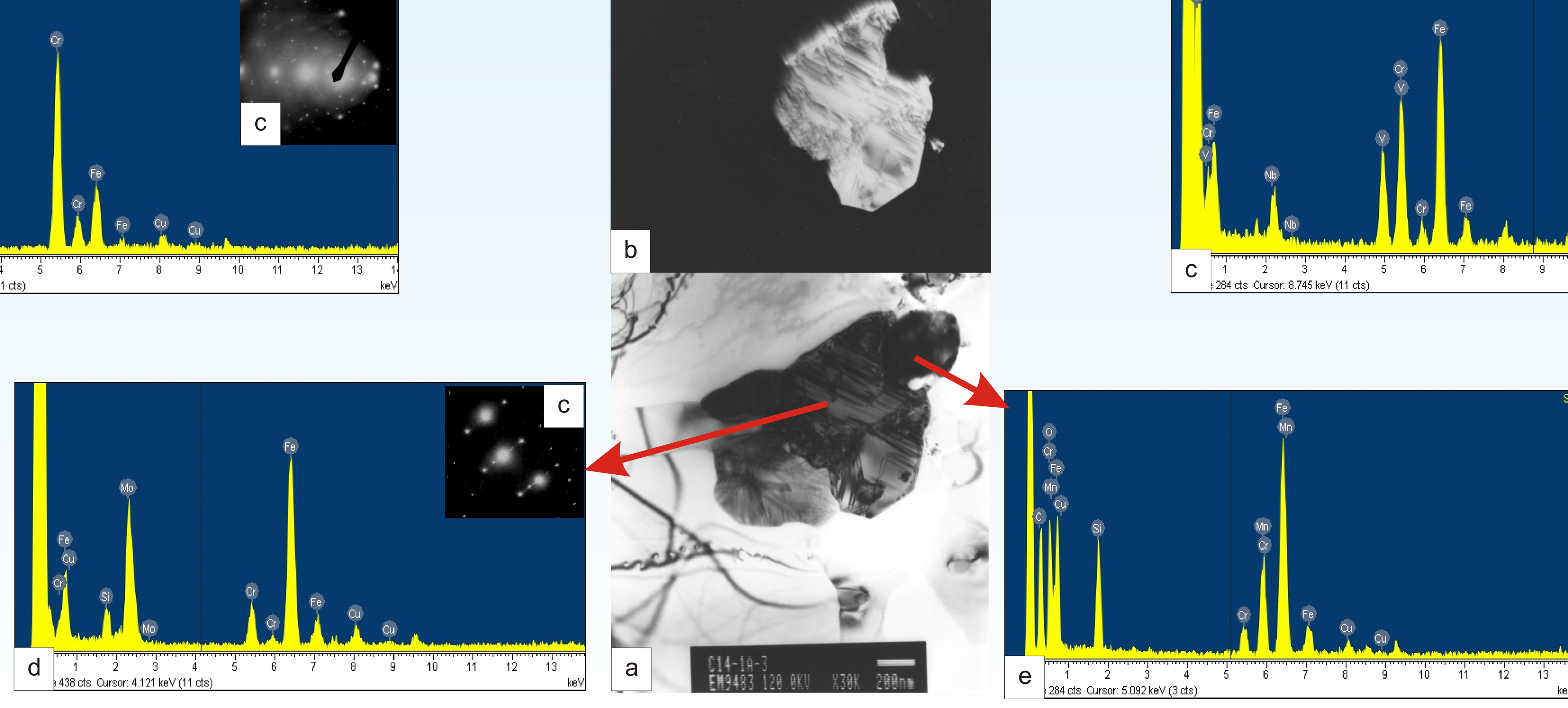

Figure 13. Cluster of particles in the weld metal of C weld joint after test 625°C/50MPa/29,312hrs: a) TEM micrograph, b) dark field image in reflection of Laves phase, c) diffraction patterns of Laves phase and d) EDX spectrum of Laves phase, e) EDX spectrum of oxide particle.

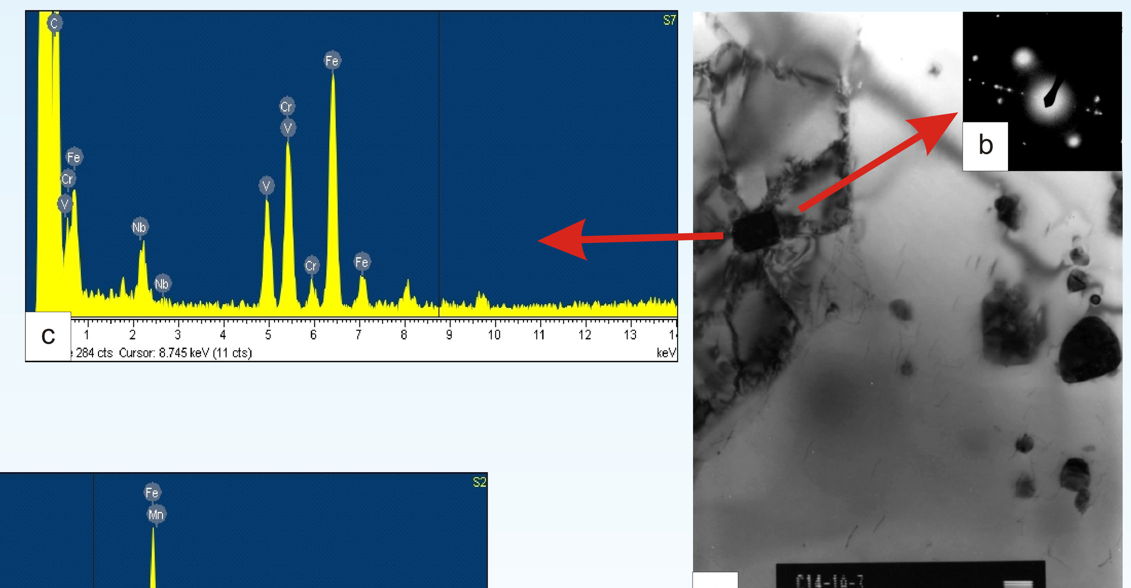

Figure 14. Coarse M23C6 carbides and particle of Z-phase (indicated with arrow) in the weld metal of C weld joint after test 625°C/50MPa/29,312hrs: a) TEM micrograph, b) diffraction patterns of Z-phase and c) EDX spectrum of Z-phase.

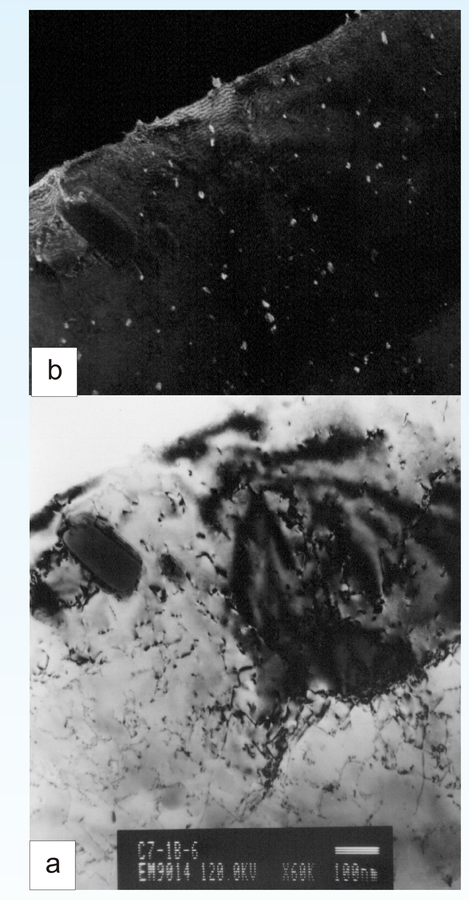

Figure 15. Fine precipitate in the base material of C weld tested at 575°C/140MPa/10,031hrs: a) bright field and b) dark field of reflection of VN nitride.